PNAS RESEARCH ARTICLE | PHYSIOLOGY

Lipid kinase PIK3C3 maintains healthy brown and white adipose tissues to prevent metabolic diseases

Wenqiang Song[a], J. Luke Postoak[a], Guan Yang[a,b], Xingyi Guo[c,d], Heather H. Pua[a], Jackie Bader[a], Jeffrey C. Rathmell[a], Hanako Kobayashi[e,f,g], Volker H. Haase[e,f,g], Katrina L. Leaptrot[h,i], Alexandra C. Schrimpe-Rutledge[h,i], Stacy D. Sherrod[h,i], John A. McLean[h,i], Jianhua Zhang[j,k], Lan Wu[a,1], and Luc Van Kaer[a,1]

Edited by Ana Maria Cuervo, Albert Einstein College of Medicine, Bronx, NY; received August 30, 2022; accepted September 29, 2022

Adequate mass and function of adipose tissues (ATs) play essential roles in preventing metabolic perturbations. The pathological reduction of ATs in lipodystrophy leads to an array of metabolic diseases. Understanding the underlying mechanisms may benefit the development of effective therapies. Several cellular processes, including autophagy and vesicle trafficking, function collectively to maintain AT homeostasis. Here, we investigated the impact of adipocyte-specific deletion of the lipid kinase phosphatidylinositol 3-kinase catalytic subunit type 3 (PIK3C3) on AT homeostasis and systemic metabolism in mice. We report that PIK3C3 functions in all ATs and that its absence disturbs adipocyte autophagy and hinders adipocyte differentiation, survival, and function with differential effects on brown and white ATs. These abnormalities cause loss of white ATs, whitening followed by loss of brown ATs, and impaired "browning" of white ATs. Consequently, mice exhibit compromised thermogenic capacity and develop dyslipidemia, hepatic steatosis, insulin resistance, and type 2 diabetes. While these effects of PIK3C3 largely contrast previous findings with the autophagy-related (ATG) protein ATG7 in adipocytes, mice with a combined deficiency in both factors reveal a dominant role of the PIK3C3-deficient phenotype. We have also found that dietary lipid excess exacerbates AT pathologies caused by PIK3C3 deficiency. Surprisingly, glucose tolerance is spared in adipocyte-specific PIK3C3-deficient mice, a phenotype that is more evident during dietary lipid excess. These findings reveal a crucial yet complex role for PIK3C3 in ATs, with potential therapeutic implications.

PIK3C3/VPS34 | autophagy | adipocyte | lipodystrophy | metabolic disease

Adipose tissues (ATs) of humans and mice appear as brown ATs (BATs) and white ATs (WATs) (1, 2). In addition to producing heat (BATs) and storing and releasing lipids (WATs), adequate mass and function of ATs play essential roles in many aspects of physiology by releasing soluble factors and extracellular vesicles (3–5). Although the underlying mechanisms differ, pathological expansion or reduction of ATs can both cause metabolic perturbations that lead to an array of metabolic diseases (6, 7). This highlights the need to understand the mechanisms that collectively maintain AT homeostasis for devising therapeutic interventions. Adipose parenchyma is comprised of brown adipocytes (BAs) in BATs and white adipocytes (WAs) in WATs (8, 9). A third adipocyte subset resembling BAs, namely beige adipocytes, is induced in WATs in response to cold exposure or sympathetic nerve stimulation (10, 11).

Pathological AT reduction is seen in lipodystrophy, a group of genetic or acquired conditions characterized by partial or generalized loss of ATs. Lipodystrophy can lead to metabolic disorders including dyslipidemia, hepatic steatosis, insulin resistance, and type 2 diabetes (T2D) (12, 13). While clinically recognized lipodystrophy is relatively rare (14), subtle forms and loss of ATs in common diseases such as cancer, HIV infection, and autoimmunity are clinically underappreciated (12, 13). Both BATs and WATs can be affected in lipodystrophy (15–17). Efforts to understand the mechanisms underlying loss of ATs have identified several critical cellular pathways, such as micro-RNA processing and autophagy.

Autophagy is a cellular process that delivers unneeded, old, and damaged cellular components for lysosomal degradation (18, 19). It also contributes to cellular functions such as lipid droplet formation/degradation, secretory vesicle formation/release, and mitochondrial maintenance/function (20–22). Although earlier studies identified autophagy as a protective mechanism against stress, it is now clear that it also controls the homeostasis of non-stressed cells (23). A series of cytoplasmic protein complexes operate sequentially during autophagy (24). Recent studies have examined several of these autophagy-related (ATG) factors in AT homeostasis, with divergent effects depending on the factor explored (25–30). The absence of ATG3, ATG16L1, Beclin1, or Rubicon in adipocytes caused loss

Significance

Uncontrolled reduction of fat tissues can cause an array of diseases that include diabetes but mechanisms remain to be fully defined. Autophagy, a cellular self-eating process, takes part in regulating the health of fat tissues. We investigated the role of an autophagy-participating factor named PIK3C3 in fat cell health and related metabolic diseases. We have found that the absence of PIK3C3 in fat cells of mice causes defects in the differentiation, survival, and function of fat cells, resulting in compromised body temperature control, abnormal blood lipid levels, fatty liver, and diabetes that resemble the abnormalities seen in patients with lipodystrophy. These findings reveal a crucial role for PIK3C3 in fat tissues, with potential therapeutic implications.

Author contributions: W.S., J.L.P., H.H.P., J.C.R., V.H.H., S.D.S., J.A.M., L.W., and L.V.K. designed research; W.S., J.L.P., G.Y., J.B., H.K., K.L.L., A.C.S.-R., and L.W. performed research; J.Z. contributed new reagents/analytic tools; W.S., J.L.P., X.G., H.H.P., J.B., J.C.R., H.K., V.H.H., K.L.L., A.C.S.-R., S.D.S., J.A.M., J.Z., L.W., and L.V.K. analyzed data; and W.S., L.W., and L.V.K. wrote the paper.

Competing interest statement: L.V.K. is a member of the scientific advisory board of Isu Abxis Co., Ltd. (South Korea). The other authors declare no competing interests.

This article is a PNAS Direct Submission.

[1]To whom correspondence may be addressed. Email: lan.wu.1@vumc.org or luc.van.kaer@vumc.org.

This article contains supporting information online at https://www.pnas.org/lookup/suppl/doi:10.1073/pnas.2214874120/-/DCSupplemental.

Published December 27, 2022.

of WATs, sometimes together with whitening of BATs, and development of metabolic disorders (25–27). However, the absence of ATG7 or ATG5 in adipocytes resulted in opposite effects, causing enhanced BATs and/or "browning" of WATs accompanied by improved systemic metabolic profile (28–30).

Phosphatidylinositol 3-kinase catalytic subunit type 3 (PIK3C3), also referred to as vacuolar sorting protein 34 (VPS34), is a lipid kinase important for cellular processes that sort cargo to lysosomes. PIK3C3 forms either complex I that produces phosphatidylinositol 3-phosphate at the phagophore to promote the formation of nascent autophagosome, or complex II that has a main role in endocytic sorting along with other cellular functions such as coordinating autophagosome maturation and endocytic trafficking (31–33). PIK3C3 is upstream of ATG7 and ATG5 in the autophagy pathway (34, 35). A previous study examined PIK3C3 in perigonadal WATs of 1- to 2-y-old mice and observed a seemingly beneficial effect on browning of this adipose depot (36). However, the role of PIK3C3 in different ATs and its impact on systemic metabolism as mice grow and mature remain unclear. Here, we targeted *Pik3c3* in adipocytes using *Adipoq-Cre*-mediated deletion (37) and found a crucial yet complex role of PIK3C3 in AT homeostasis and systemic metabolism.

Results

Adipocyte-Specific Deletion of *Pik3c3* Disturbs Autophagy and Causes Generalized Lipodystrophy. We generated *Adipoq-Cre*;*Pik3c3*$^{f/f}$ (cKO) and *Pik3c3*$^{f/f}$ [wild-type (WT)] mice and analyzed interscapular BAT (iBAT), inguinal subcutaneous WAT (iWAT), and visceral perigonadal WAT (pWAT: epididymal in males and periovarian in females) (*SI Appendix*, Fig. S1*A*). PIK3C3 messenger RNA (mRNA) and protein were detected in all three depots of WT mice and were significantly reduced in cKO mice (Fig. 1*A* and *SI Appendix*, Fig. S1*B*). The deletion of *Pik3c3* was adipocyte specific, as the levels of its protein as well as the autophagosome cargo protein P62 were not affected in liver, heart, and lung (*SI Appendix*, Fig. S1*C*). The impact on autophagy was detected in all three depots of cKO mice, reflected by levels of microtubule-associated proteins 1A/1B light chain 3B (LC3)-I, LC3-II, and P62 proteins that were increased or trended higher (Fig. 1*B* and *SI Appendix*, Fig. S1*B*). We also detected increased levels of lysosomal-associated membrane protein 1 (LAMP1) that is important for fusion of autophagosomes with lysosomes to generate autophagolysosomes (Fig. 1*B* and *SI Appendix*, Fig. S1*B*). In evaluating autophagic flux, we observed significantly decreased LC3-II response to lysosomal inhibition in iWAT and pWAT of cKO mice, indicating impaired autophagy (Fig. 1*C* and *SI Appendix*, Fig. S1*D*). Such a defect was not observed in iBAT of cKO mice (Fig. 1*C*); however, compared with iWAT and pWAT, the response of iBAT to autophagy inhibition reagents was incomplete (*SI Appendix*, Fig. S1*D*). We then used the autophagy reporter strain CAG-RFP-EGFP-LC3 to generate *Rosa26-Cre*^{ERT2};*Pik3c3*$^{f/f}$;CAG-RFP-EGFP-LC3 mice, and in vitro differentiated preadipocytes isolated from iBAT and iWAT. We detected stronger RFP signals in *Pik3c3*-deleted cells, consistent with increased LC3 levels in ATs of cKO mice (Fig. 1*D*). Upon deletion of *Pik3c3*, maturation of autophagosomes and fusion with lysosomes were lower in adipocytes from both iBAT and iWAT when cells were cultured in the absence or presence of serum, confirming impaired autophagy in both AT depots (Fig. 1*E*). Combined with the results showing LAMP1 accumulation, these data implicate defective autophagosome maturation and fusion of autophagosomes with lysosomes as an outcome of PIK3C3 deficiency in adipocytes. These results indicate that *Adipoq-Cre*-mediated deletion specifically diminishes PIK3C3 and disturbs autophagy in adipocytes.

We examined AT mass, morphology, and histology in mice from postnatal (P) day 1 (P1) to 24 wk (W24) of age. iBAT was dissectible at P1 although lipid deposition was minimal in both WT and cKO mice (*SI Appendix*, Fig. S1*E*). Excessive lipid accumulation was observed at postnatal day 10 (P10) that became progressively more pronounced at W4 and W8 in cKO mice, evidenced by larger lipid droplets, less brown appearance, and increased tissue weight (Fig. 1*F* and *SI Appendix*, Fig. S1*E*). As mice became older, the weight differences in iBAT gradually reversed reaching statistical significance at W24 (Fig. 1*F*). The remaining adipocytes in iBAT of cKO mice at W24 contained primarily large lipid droplets and lacked multilocular characteristics (*SI Appendix*, Fig. S1*E*). As such, PIK3C3 deficiency in BAs causes BAT whitening in young mice and BAT loss in older mice. iWAT was also readily dissectible at P1 with minimal lipid deposition (*SI Appendix*, Fig. S1*E*). Unilocular WAs were abundant at P10 in both groups of mice. Thereafter, iWAT progressively became smaller in cKO mice (Fig. 1*F* and *SI Appendix*, Fig. S1*E*). pWAT was not reliably dissectible at P1 and P10 of either genotype. As mice became older, alterations in this depot mostly resembled, although lagged behind, alterations seen in iWAT (Fig. 1*F* and *SI Appendix*, Fig. S1*E*). Both iWAT and pWAT of W8 cKO mice contained more small-sized adipocytes but fewer medium-sized adipocytes, but there was no significant difference in large-sized adipocytes between the two genotypes although some could be observed in cKO mice (*SI Appendix*, Fig. S1 *E* and *F*). Combined with the findings discussed below, these results are consistent with a compensatory increase in the generation of preadipocytes that fail to fully differentiate. As such, PIK3C3 deficiency in WAs causes progressive loss of WATs. The enlarged interstitial areas in iBAT and iWAT of older cKO mice (*SI Appendix*, Fig. S1*E*), at least partially, were due to the deposition of excessive extracellular matrix as evidenced by increases in collagens (Fig. 1*G*). Together, these findings demonstrate that adipocyte-specific deletion of *Pik3c3* progressively affects AT mass, morphology, and histology with differential impact on BATs and WATs. We obtained consistent results for males and females, and tissue weights for mice at W24 are shown in *SI Appendix*, Fig. S1*G*.

Body weight was not affected in either males or females at the age examined (*SI Appendix*, Fig. S2*A*). Consistent with dynamic alterations in iBAT weight, the ratio of its depot to body weight decreased only in older cKO mice (*SI Appendix*, Fig. S2*B*). Food intake was comparable between WT and cKO mice at younger age whereas the latter group appeared to consume more food at older age (*SI Appendix*, Fig. S2*C*). While the underlying reason is unclear, we speculate that the reduced capacity of maintaining body temperature becomes more profound in older cKO mice that require more food intake for heat generation. The progressive loss of ATs in cKO mice was accompanied by the development of insulin resistance that proceeded to T2D (Fig. 2 *A* and *B*). However, the results from intraperitoneal insulin tolerance test (IPITT) and glucose tolerance test (IPGTT) diverged. IPGTT at W24 revealed hyperglycemia before and 3 h after the glucose load, indicative of diabetes, with blood glucose levels appearing lower upon glucose challenge in cKO mice (Fig. 2*C*). Again, we obtained consistent results from glucose and insulin tolerance tests in males and females, although the phenotype of the latter appeared somewhat more severe (see *Results* for W24 in *SI Appendix*, Fig. S2 *D* and *E*). cKO mice also developed dyslipidemia as revealed by hypotriglyceridemia at the fasting state and a trend toward hypertriglyceridemia at the fed state, indicating

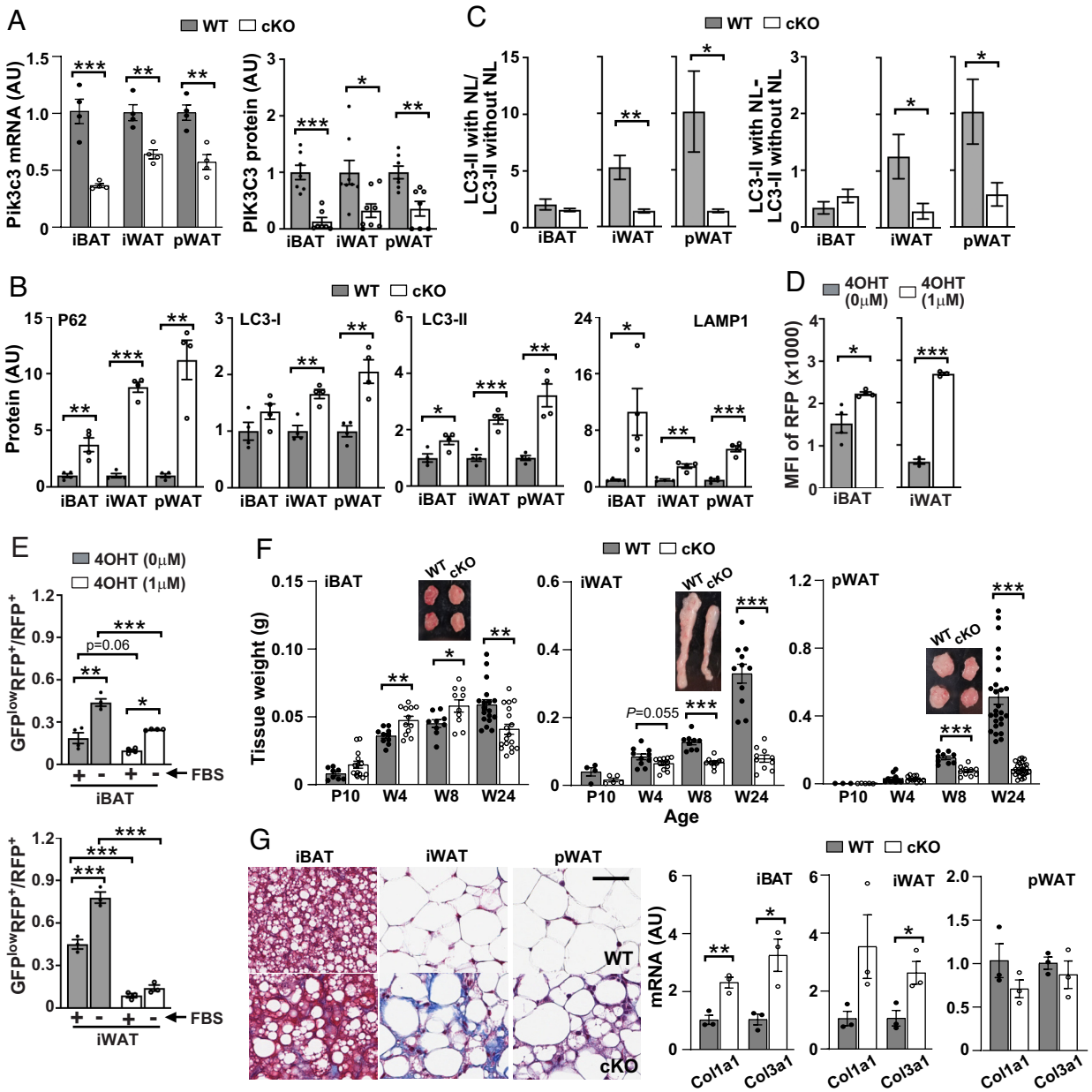

Fig. 1. Adipocyte-specific deletion of *Pik3c3* disturbs autophagy and causes generalized lipodystrophy. Mice at W8 and W24 were used except for *F*. *A* and *B*. PIK3C3 mRNA and protein (*A*), P62, LC3, and LAMP1 protein (*B*) were examined (n = 4 to 8 in each group). *C*. Autophagic flux (LC3-II with inhibitor/LC3-II without inhibitor, *Left* and LC3-II with inhibitor—LC3-II without inhibitor, *Right*) was evaluated (n = 6 to 13 in each group). *D* and *E*. RFP representing LC3 (*D*) and autophagy progression (*E*) were examined (n = 3 to 4 in each group). *F*. Mice at the specified age were examined (n = 3 to 26 in each group at each time point). *G*. Collagen proteins (*Left*) and mRNAs (*Right*) were examined (n = 3 in each group). (Scale bar, 100 μm.) AU: arbitrary unit; NL: NH_4Cl + leupeptin.

reduced capacity to store and release lipids (Fig. 2*D*). Ectopic lipid deposition was detected in older cKO mice, reflected by increased liver lipids (Fig. 2*E*).

Together, these results demonstrate that PIK3C3 deficiency in murine adipocytes causes progressive loss of all ATs and development of metabolic disorders that resemble those found in humans with generalized lipodystrophy. The early increased mass of BAT is accompanied by excessive lipid deposition. Our subsequent studies investigated the underlying mechanisms focusing on mice at W8 and W24. The results of these mechanistic studies are presented as combined data from both sexes.

Deletion of *Pik3c3* Impairs Adipocyte Differentiation, Survival, and Function. We first quantified preadipocytes (*SI Appendix*, Fig. S3*A*) (38). Akin to lipodystrophic A-Zip mice (38, 39), subsets of preadipocytes were higher or trended higher in cKO mice at W24 when the mass of all three depots was reduced (Fig. 3*A*), making it unlikely that defects in preadipocyte generation contribute to AT loss. We next assessed adipocyte differentiation (40, 41). We expanded preadipocytes from stromal vascular fraction (SVFs) and cultured those from iBAT under BA differentiation conditions (41) and those from iWAT under BA or WA differentiation conditions (40). In comparing WT and cKO mice, we found fewer lipid-containing adipocytes in cultures of iBAT from W8 cKO mice that accumulated fewer lipids (Fig. 3*B* and *SI Appendix*, Fig. S3*B*). Such impaired differentiation was not consistently observed in cultures of iWAT from cKO mice at this age (*SI Appendix*, Fig. S3*C*). These findings indicate that PIK3C3 promotes preadipocyte differentiation, at least in BATs. Together with the results on

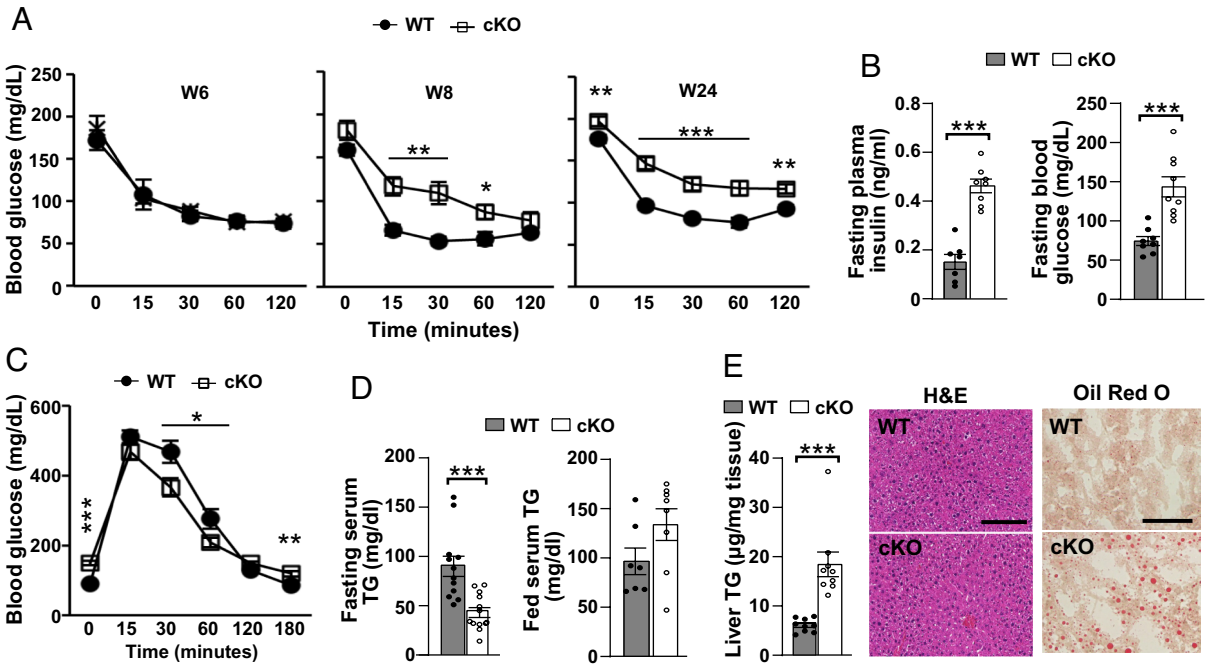

Fig. 2. Adipocyte-specific deletion of *Pik3c3* causes metabolic disorders. Mice at W24 were used except for *A*. *A*. IPITT was performed on mice at the indicated age (n = 7 to 19 in each group at each age). *B*. Fasting blood glucose and plasma insulin were examined (n = 7 to 9 in each group). *C*. IPGTT was performed (n = 15 to 21 in each group). *D*. Serum lipids were examined (n = 7 to 12 in each group). *E*. Liver lipids (*Left*, n = 8 to 9 in each group), H&E-stained (*Middle*, scale bar, 100 μm), and Oil red O-stained (*Right*, scale bar, 50 μm) liver sections (n = 4 in each group) were examined.

adipocyte size measurements shown in *SI Appendix*, Fig. S1*F*, the higher fractions of preadipocytes in cKO mice could represent a compensatory response to loss of ATs and/or an impaired ability of these cells to differentiate. We detected significantly higher levels of cleaved Caspase-3 (CASP3) in ATs of W8 cKO mice (Fig. 3*C* and *SI Appendix*, Fig. S3*D*), indicating that cell death contributes to loss of ATs in cKO mice.

To assess the function of ATs, we first measured selected markers reflective of lipid metabolism. These included mRNAs for pathways of substrate uptake, lipogenesis, and lipolysis, and proteins for adipogenesis, lipogenesis, and lipid droplet formation (*SI Appendix*, Tables S1 and S2). Consistent with the above-described morphological changes in W8 cKO mice, levels of these markers were impacted in all three depots but to different degrees with the most widespread decreases in iBAT (Fig. 3 *D* and *E* and *SI Appendix*, Fig. S3*D*). We performed additional analyses of mRNAs for pathways of β-oxidation, uncoupling of β-oxidation from ATP synthesis, and thermogenesis, and protein levels of the critical thermogenesis factor uncoupling protein 1 (UCP1) (*SI Appendix*, Tables S1 and S2) (29, 30, 42). Except for *Ppargc1a*, these markers were significantly reduced in iBAT of cKO mice (Fig. 3 *F* and *G* and *SI Appendix*, Fig. S3*D*). We were unable to reliably detect UCP1 protein in iWAT and pWAT from either WT or cKO mice (*SI Appendix*, Fig. S3*D*). However, mRNA levels for *Ucp1* as well as the β-oxidation genes peroxisome proliferator activated receptor alpha (*Ppara*) and acyl-coA dehydrogenase long chain (*Acadl*) were significantly higher in pWAT and trended higher in iWAT of W8 cKO mice, implicating upregulation of certain mitochondrial components (Fig. 3*H*). We also measured mRNA levels of selected cytokines/adipokines, which revealed the most significant decreases in several adipokines in iBAT of cKO mice (Fig. 3*I*). Interestingly, we detected significant upregulation of fibroblast growth factor 21 (*Fgf21*), a factor participating in interorgan communication to maintain energy homeostasis (43), in iBAT and pWAT of cKO mice (Fig. 3*I*).

We employed ex vivo assays to further evaluate AT function. The examination of mitochondrial respiration yielded results in iBAT divergent from those in iWAT and pWAT, with the former trending lower and the latter two trending higher in cKO mice (*SI Appendix*, Fig. S4*A*). Lipolysis in response to isoproterenol stimulation also appeared different among the depots, with decreases in iWAT and pWAT but not in iBAT of cKO mice (*SI Appendix*, Fig. S4*B*). Untargeted lipidomic analyses to assess the lipid profiles in iBAT and pWAT detected over 4,000 compounds in each depot (Dataset S1) and deletion of *Pik3c3* changed the lipidome of both depots in cKO mice (Fig. 4*A*). Although the overall lipid profile or signature of pWAT remained distinct from that of iBAT, the former moved closer to the latter in cKO mice, indicative of fewer lipid differences (Fig. 4*A*). Statistically significant lipid species ($P < 0.05$ and fold change ≥ 1.5) between WT and cKO mice for iBAT and pWAT were annotated and tagged as differentially abundant lipids (DAL, Dataset S3). Volcano plots indicate that numerous lipid species were observed to change in the untargeted lipidomic approach (Fig. 4*B*). In particular, fewer triglycerides (TG) in both depots of cKO mice were consistent with loss of ATs, whereas accumulation of diglycerides may be reflective of impaired re-esterification (Fig. 4*B*). These data also show that fewer glycerophospholipids (lysophosphatidylcholine, lysophosphatidylethanolamine, phosphatidylcholine, phosphatidylethanolamine, phosphatidylglycerol, and phosphatidylinositol) but more TG (56:7), TG (56:8), TG (58:10), TG (58:8), TG (58:9), TG (61:8), TG (64:8), and TG (69:15) were detected in iBAT of cKO mice (Fig. 4*B*). Alterations in glycerophospholipids in pWAT displayed a distinct pattern, which was increased in cKO mice (Fig. 4*B*). Most notably and contrary to iBAT, the mitochondrial-specific cardiolipins (CL) were increased in pWAT of cKO mice (Fig. 4*B*). Together with our analyses of mRNAs (Fig. 3*H*) and mitochondrial respiration (*SI Appendix*, Fig. S4*A*), these findings support the notion that PIK3C3 deficiency differentially impacts BATs and WATs with impaired mitochondria in the

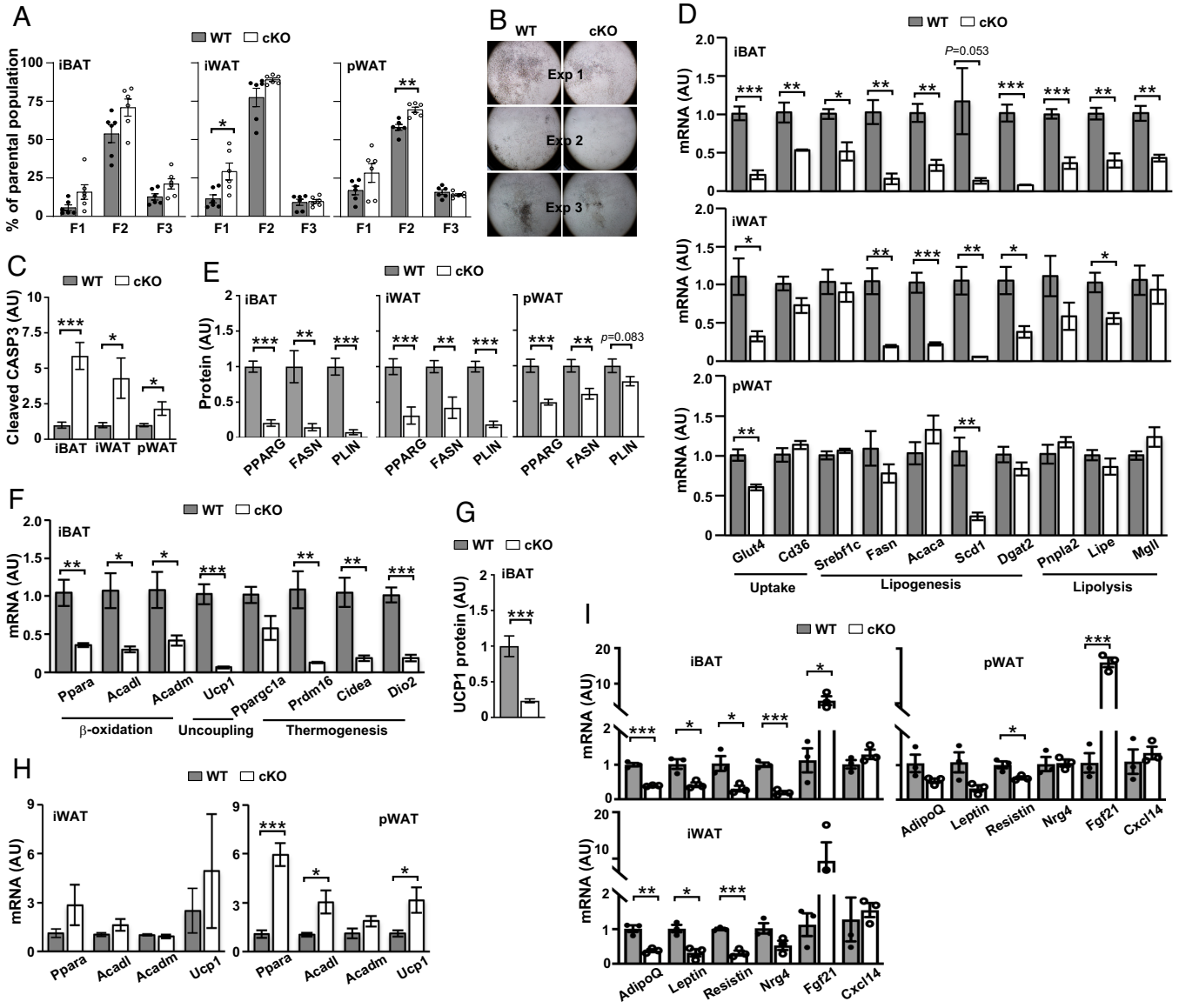

Fig. 3. Adipocyte-specific deletion of *Pik3c3* impairs adipocyte differentiation, survival, and function. *A*. SVFs were analyzed by flow cytometry for preadipocytes fraction F 1 to 3 (n = 6 in each group). *B*. Preadipocytes from iBAT were in vitro differentiated and stained with Oil red O (n = 3 in each group). *C*. CASP3 was examined by western blotting. Band intensity was quantified to reflect protein level. *D–I*. The indicated mRNAs or proteins (quantification of band intensity) were examined in mice at W8 (n = 3 to 7 in each group for mRNAs and n = 7 to 8 in each group for proteins).

former but enhanced mitochondria in the latter. Lastly, DALs were uploaded into the lipid pathway enrichment analysis (LIPEA) algorithm for pathway enrichment analysis, and the data revealed significantly affected pathways including autophagy, glycerophospholipid metabolism, and cell death (Fig. 4*C*).

Considering the function of ATs in releasing small RNAs (sRNAs) that participate in inter-organ communication (4, 6), we examined circulating sRNAs by sRNA sequencing. We observed significant differences in length distributions between WT and cKO mice with a decreased pattern for sRNAs of 22 nucleotides or shorter in the latter (Fig. 4*D*, chi-squared test $P < 2.2e{-}16$). We annotated different classes of sRNAs (Dataset S3). While the proportions of different classes of sRNAs were not significantly different between WT and cKO mice (*SI Appendix*, Fig. S4*C*), the number of reads with architectural features of PIWI-interacting RNAs in the unmapped proportion was increased in cKO mice (*SI Appendix*, Fig. S4*D*). The differential expression analysis using the criteria of $P < 0.05$ and fold change ≥ 1.5 identified 42 differentially expressed sRNA (DES) with 20 upregulated and 22 downregulated in cKO mice (Fig. 4*E*). These results indicate that adipocyte-specific *Pik3c3* deletion alters the circulating sRNA pool.

The above findings demonstrate that PIK3C3 promotes adipocyte differentiation, survival, and function. Consistent with the observations for adipocyte mass, morphology, and histology, the functional analyses reveal a differential impact of PIK3C3 deficiency on BATs and WATs that is particularly evident in mitochondria.

Adipocyte-Specific Deletion of *Pik3c3* Compromises Thermogenesis. Non-shivering thermogenesis participates in maintaining body temperature, in particular, under extreme conditions such as cold and starvation, which is primarily a function of BATs (44, 45). We therefore examined thermogenesis. To exclude confounding factors, we first measured several metabolic parameters in mice housed at room temperature (25 °C) with food and water ad lib. We found comparable body weight but reduced total body fat in cKO mice (*SI Appendix*, Fig. S5*A*). Under these conditions, WT and cKO mice had similar oxygen consumption (VO_2), carbon

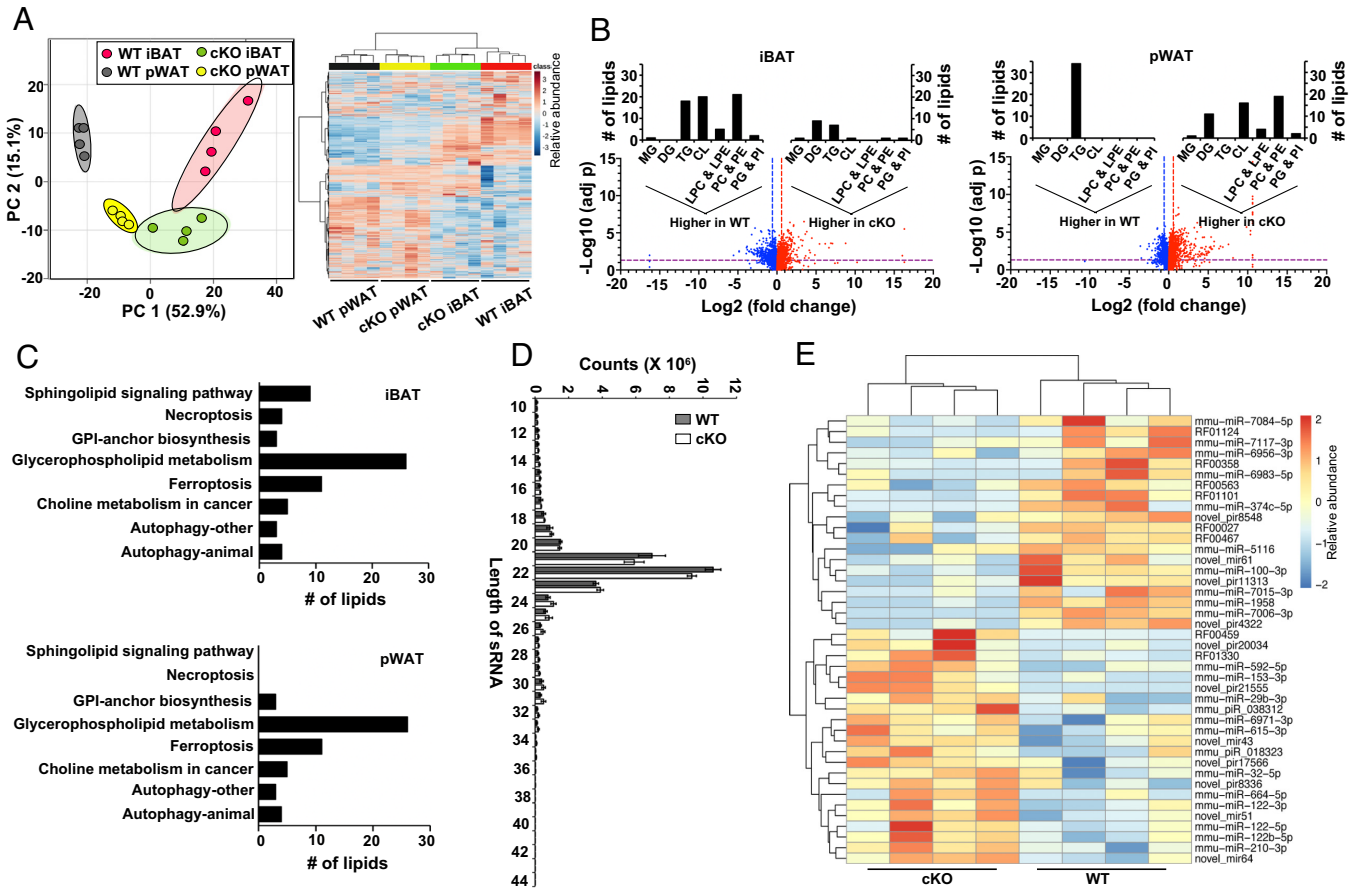

Fig. 4. Adipocyte-specific deletion of *Pik3c3* alters AT lipidome and circulating sRNA. Mice at W24 were used. *A–C*. Global untargeted lipidomics was performed. Shown are PCA and heatmap (*A*), DALs (*B*), and affected pathways (*C*, GPI: glycosylphosphatidylinositol) with n = 4 in each group. *D* and *E*. sRNAs in plasma were analyzed by sRNA sequencing. Shown are the length distribution (*D*) and heatmap using TPM of DESs (*E*) with n = 4 in each group.

dioxide production (VCO_2), energy expenditure (*SI Appendix*, Fig. S5*B*), and body temperature (Fig. 5*A*). After exposure to cold (6 °C) for 1 wk with food and water ad lib, both groups of mice similarly maintained intrarectal and iBAT temperature and gained comparable body weight (Fig. 5*A* and *SI Appendix*, Fig. S5*C*). We measured selected markers in iBAT, including mRNA for *Ucp1* as well ascell death inducing DFFA like effector a (*Cidea*), and protein for UCP1, fatty acid synthase (FASN), and peroxisome proliferator activated receptor gamma (PPARG), which revealed impaired responses in cKO mice (Fig. 5*B*). As such, cKO mice can sustain body temperature upon cold exposure for a week in the face of a compromised thermogenic response. To explore whether this remains true under harsher conditions, we deprived food during cold exposure for 6 h. Such treatment promoted autophagy in iBAT of WT mice, reflected by increases in LC3-II and significantly increased LC3-II to -I ratio (Fig. 5*C* and *SI Appendix*, Fig. S5*D*) (46). Whereas intrarectal and iBAT temperature were maintained as expected during cold treatment alone in both groups (*SI Appendix*, Fig. S5*E*), superimposing food deprivation readily unmasked defective thermogenesis in cKO mice accompanied by near absence of the examined markers in iBAT (Fig. 5*D*). Together, the above findings demonstrate that PIK3C3 deficiency in adipocytes compromises thermogenic capacity of BATs that affects body temperature under extreme conditions.

Beige adipocytes are induced in WATs, most commonly examined in iWAT, in response to cold or sympathetic nerve stimulation. These browning or "beiging" ATs can also participate in thermogenesis (47). As such, we evaluated the browning response in iWAT. In the above experiments with cold treatment for 1 wk, we did not observe significant upregulation of the examined markers in iWAT of WT mice, whereas the marker proteins were nearly undetectable in iWAT of cKO mice (*SI Appendix*, Fig. S5*F*). We then assessed the response to sympathetic nerve stimulation, applying β3-adrenergic receptor agonist Cl316243 to mice for 1 wk. In addition to the above-selected markers, we measured mRNA for several markers characteristic of iWAT browning. The results showed a significantly dampened response in iWAT of cKO mice (Fig. 5*E*).

Together, these findings further support a crucial role of PIK3C3 in promoting BATs.

Deletion of *Pik3c3* in Adipocyte Cell Line Mirrors the Findings in cKO Mice. To examine adipocytes in isolation, we employed cell line models (Fig. 6*A*). We generated brown preadipocytes immortalized *Adipoq-Cre* (IAC)-BAT and immortalized *Rosa26-Cre* (IRC)-BAT using distinct inducible Cre/loxP systems (see *Materials and Methods*). We first cultured IAC-BAT cells under BA differentiation conditions, which revealed their capacity to differentiate into BAs (*SI Appendix*, Fig. S6*A*). PIK3C3 was upregulated and so were ATG7 and Rubicon, whereas P62 and LC3 were reduced, perhaps reflecting an accelerated autophagy during differentiation (*SI Appendix*, Fig. S6*B*). We then induced excision of *Pik3c3* in IAC-BAT cells using 4-hydroxytamoxifen (4OHT) during differentiation, which significantly reduced its mRNA and protein (Fig. 6 *B* and *C*). Consistent with our findings in cKO mice, this caused the following dose-dependent alterations: 1) increased P62, LC3, LAMP1, and cleaved Caspase 3, and decreased UCP1, PPARG, and FASN

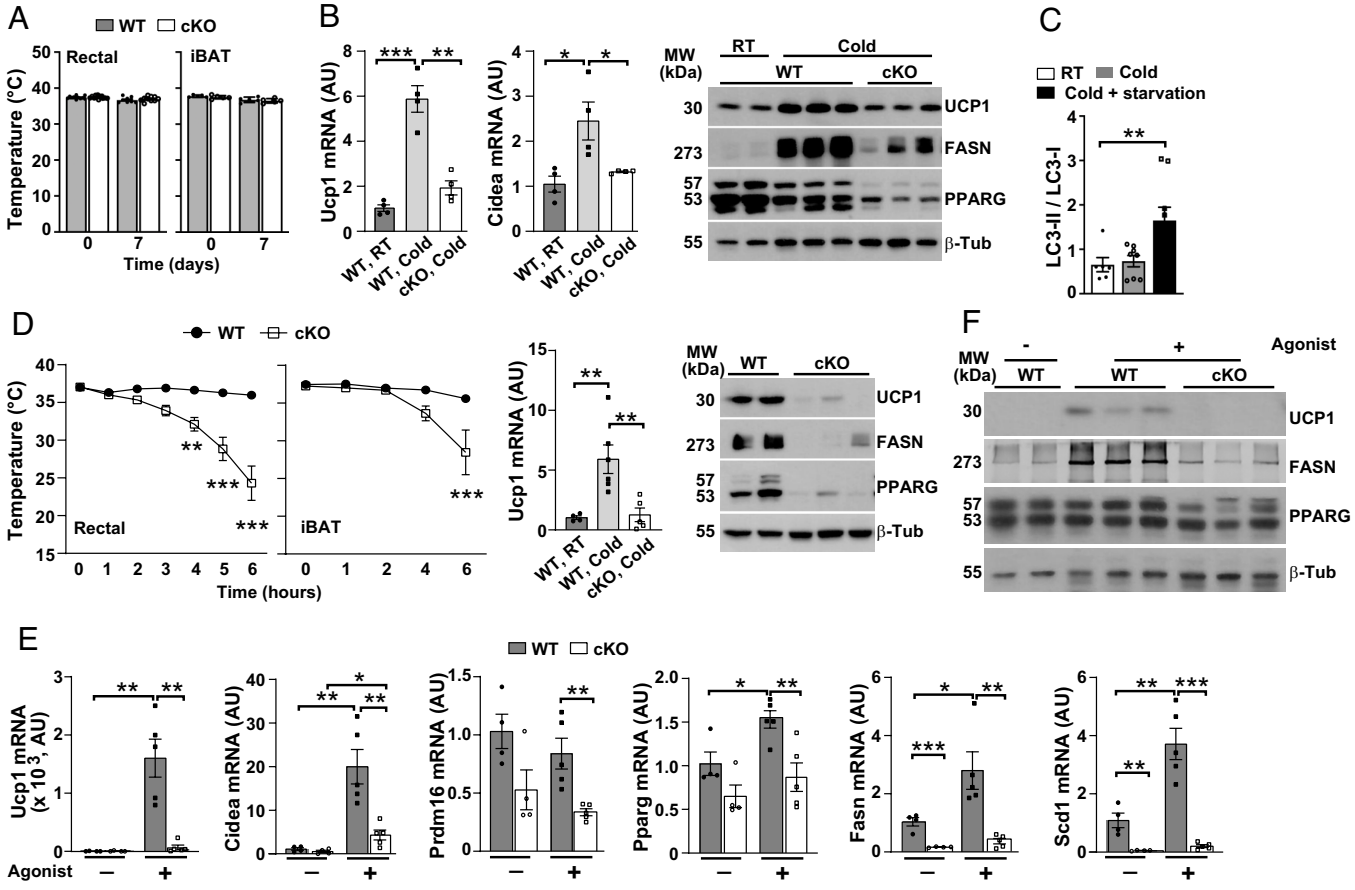

Fig. 5. Adipocyte-specific deletion of *Pik3c3* compromises thermogenic response. Mice at W8 were used. *A*. Mice were housed at 6 °C for 1 wk with free access to food and water. Body temperature was measured (n = 5 to 13 in each group). *B*. iBAT was analyzed for indicated mRNAs and proteins (n = 2 to 4 in each group). *C*. WT mice were housed as indicated for 6 h and analyzed for LC3 II/LC3 I in iBAT by western blotting (n = 6 to 9 in each group). *D*. Mice were housed at 6 °C with free access to only water. Body temperature was recorded (n = 6 to 9 in each group). iBAT was analyzed for indicated mRNAs and proteins (n = 2 to 5 in each group). *E* and *F*. Mice were treated as indicated. iWAT was analyzed for the indicated mRNAs and proteins (*n* = 2 to 5 in each group).

(Fig. 6*C*); 2) increased apoptosis (Fig. 6*D*); and 3) reduced lipid accumulation (Fig. 6*E*). In this model, with only days of adipocyte differentiation and *Pik3c3* deletion, we detected increased mitochondrial mass (Fig. 6*F*). We obtained results from IRC-BAT cells similar to those from IAC-BAT cells (*SI Appendix*, Fig. S6 *C–E*). However, basal oxidative respiration was impaired in differentiated and PIK3C3-deficient IRC-BAT cells, consistent with the studies in iBAT of cKO mice (*SI Appendix*, Fig. S6*F*). It is unclear whether increased mitochondrial mass in these cells accounted for the observed increase in maximal oxidative respiration (*SI Appendix*, Fig. S6 *E* and *F*). We further evaluated autophagy and endocytosis/vesicle trafficking in IRC-BAT cells. Consistent with the findings in ATs of cKO mice, we observed impaired autophagy whereas epidermal growth factor receptor degradation and dye quenched-bovine serum albumin assays revealed limited defects in endocytosis and endosomal/lysosomal trafficking in differentiated PIK3C3-deficient IRC-BAT cells (Fig. 6*G* and *SI Appendix*, Fig. S6*G*). We used 3T3-L1 cells to study white preadipocytes. We cultured cells under WA differentiation conditions, which resulted in WAs with upregulation of PIK3C3 as well as P62 and LC3 (*SI Appendix*, Fig. S6*H*). We then deleted *Pik3c3* in 3T3-L1 cells employing CRISPR/Cas9 approach and cultured the resulting lines under WA differentiation conditions. This caused decreases in PIK3C3 as well as alterations similar to those seen in brown preadipocytes, including: 1) increased P62 and LC3; 2) reduced levels of markers indicative of adipocyte function; and 3) decreased lipids in differentiated adipocytes (Fig. 6 *H–J*). Results for oxidative respiration, autophagic flux, and endocytosis/vesicle trafficking were consistent with those seen in brown preadipocytes (Fig. 6*K* and *SI Appendix*, Fig. S6 *I* and *J*).

Overall, the results from adipocyte cell lines mirror those from cKO mice. Together, they demonstrate a crucial adipocyte-intrinsic role of PIK3C3 in promoting differentiation, survival, and function of BAs and WAs. They also indicate that PIK3C3 deficiency disturbs autophagy in adipocytes with more limited effects on endocytosis and endosomal trafficking.

Inducible Deletion of *Pik3c3* in Adipocytes Reproduces Findings in cKO Mice. In the cKO model, *Pik3c3* is excised during adipocyte differentiation when ADIPOQ begins to express. To investigate whether deletion of *Pik3c3* in differentiated adipocytes similarly affects ATs, we generated *Adipoq-Cre*^{ERT2};*Pik3c3*$^{f/f}$ (iKO) and *Pik3c3*$^{f/f}$ (WT) mice. We treated mice with tamoxifen (Tam) and analyzed them at W3 and W6 thereafter. As anticipated, Tam treatment reduced PIK3C3 in ATs of iKO mice (*SI Appendix*, Fig. S7 *A* and *B*). Observations in this model are consistent with those seen in cKO mice, including: 1) disturbed autophagy in AT depots of iKO mice (*SI Appendix*, Fig. S7*B*); 2) comparable body weight and food intake between WT and iKO mice (*SI Appendix*, Fig. S7*C*); 3) changes in AT mass with early increased mass of iBAT and reduced mass of iWAT and pWAT in iKO mice (*SI Appendix*, Fig. S7*D*); and 4) changes in markers for AT function, more so in iBAT than pWAT (*SI Appendix*, Fig. S7*E*). The consistent findings between cKO and iKO models reiterate the crucial role of PIK3C3 not only for differentiation but also maintenance of adipocytes.

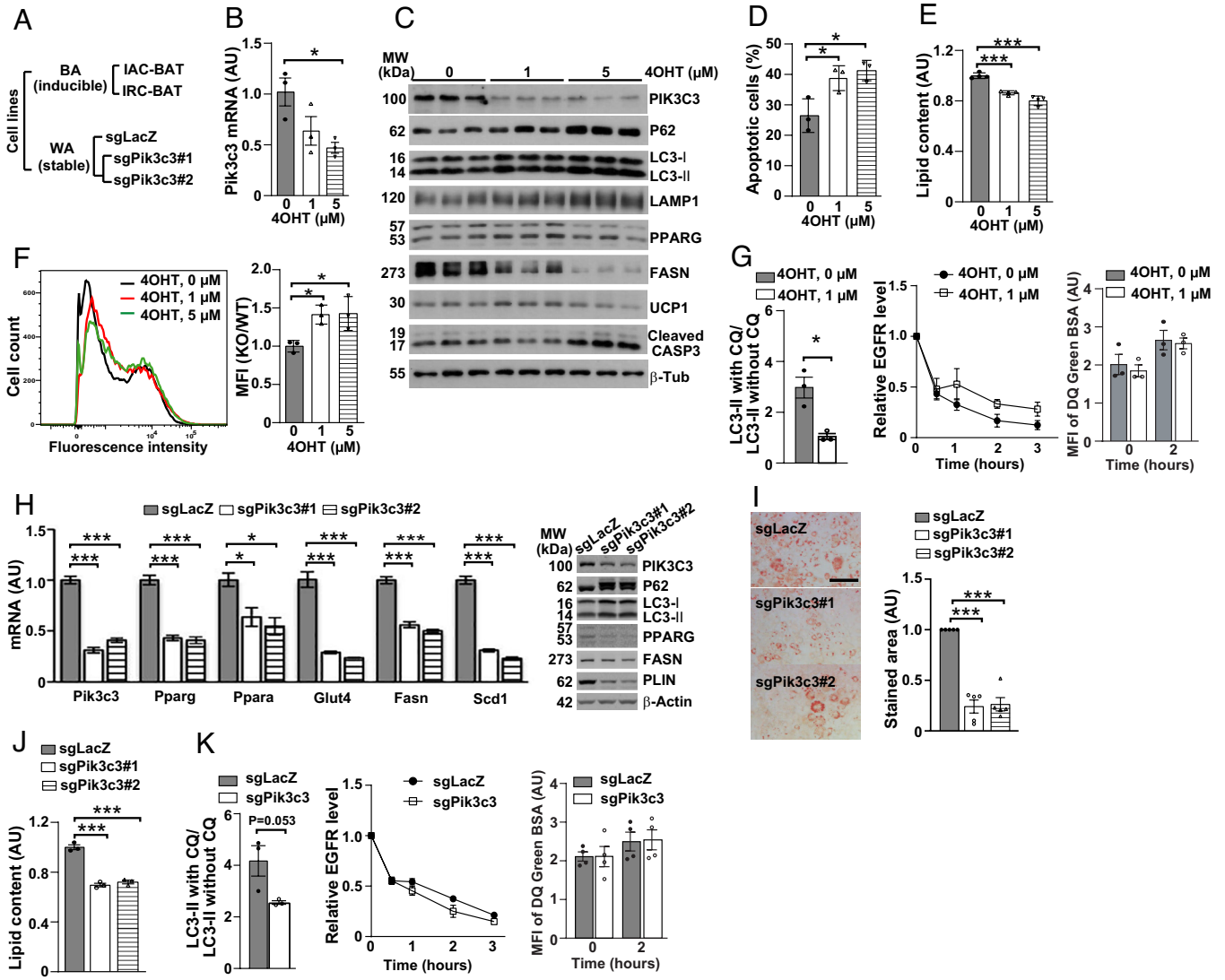

Fig. 6. *Pik3c3*-deleted preadipocyte cell lines mirror ATs of cKO mice. *A*. Cell line models are listed. *B–F*. IAC-BAT cells were induced to delete *Pik3c3* during differentiation and analyzed on day 10 for *Pik3c3* mRNA (*B*), the indicated proteins (*C*), apoptotic cells (*D*), lipid content (*E*), and mitochondrial content (*F*, MFI: mean fluorescence intensity) with n = 3 in each group. *G*. IRC-BAT cells were induced to delete *Pik3c3*, differentiated, and analyzed for autophagic flux and endocytosis/vesicle trafficking (n = 3 in each group). *H–K*. Control and *Pik3c3*-deleted 3T3-L1 cells were differentiated and analyzed on day 6 for indicated mRNAs and proteins (*H*), Oil red O staining (*I*, scale bar, 100 μm), lipid content (*J*), autophagic flux and endocytosis/vesicle trafficking (*K*) with n = 2 to 5 in each group. CQ: chloroquine.

Opposing Roles of PIK3C3 and ATG7 with a Dominant Effect of PIK3C3 Deficiency. Previous studies reported that adipocyte deletion of *Atg7* with aP2(*Fabp4*)-*Cre* transgene (aP2cKO^{Atg7}) causes changes in ATs that are beneficial to systemic metabolism, exemplified by enlarged but not whitened iBAT and decreased as well as browning of pWAT (29, 30). Because these findings are largely opposite to our observations in *Pik3c3* KO mice, we evaluated the interplay between these two factors in maintaining AT homeostasis. We generated *Adipoq-Cre*;*Atg7*$^{f/f}$ (cKO^{Atg7}) and *Adipoq-Cre*;*Pik3c3*$^{f/f}$;*Atg7*$^{f/f}$ [double knockout (DKO)] mice. In line with the analysis in aP2cKO^{Atg7} mice, this set of studies focused on iBAT and pWAT to facilitate valid comparisons. PIK3C3 was diminished in both depots of DKO but not in those of cKO^{Atg7} mice (*SI Appendix*, Fig. S8*A*). As expected, ATG7 was significantly decreased in both depots of cKO^{Atg7} mice (Fig. 7*A* and *SI Appendix*, Fig. S8*A*). Surprisingly, the levels of ATG7 trended higher in both depots of cKO mice, were reduced in pWAT of DKO mice, but were not substantially affected in iBAT of DKO mice (Fig. 7*A* and *SI Appendix*, Fig. S8*A*). While the underlying mechanism remains unclear, the deletion of *Pik3c3* could induce a compensatory increase of ATG7 in cKO^{Atg7} mice that might account for the detected ATG7 in DKO mice, possibly in concert with incomplete Cre-mediated deletion. Nevertheless, the deletion of the respective factor(s) disturbed autophagy with differential patterns on P62, LC3, and LAMP1 in the two depots. Similar to those reported for aP2cKO^{Atg7} mice (29, 30), LC3-II was significantly lower in iBAT and trended lower in pWAT of cKO^{Atg7} but this became less evident in DKO mice (Fig. 7*A* and *SI Appendix*, Fig. S8*A*). Additionally, cKO^{Atg7} mice lacked LAMP1 accumulation that was reversed in DKO mice (Fig. 7*A* and *SI Appendix*, Fig. S8*A*). Body weights were comparable among WT, cKO^{Atg7}, and DKO mice (*SI Appendix*, Fig. S8*B*). For cKO^{Atg7} mice, this was divergent from aP2cKO^{Atg7} strain that had reduced body weight (29, 30). Despite this difference, cKO^{Atg7} mice displayed alterations in iBATs that largely resembled those reported for aP2cKO^{Atg7} mice, including: 1) increased iBAT mass (Fig. 7*B*); 2) histological appearance that was similar to WT but different from cKO mice (*SI Appendix*, Fig. S8*C*); 3) unaltered or better-preserved expression of marker genes for lipid metabolism and thermogenesis compared to cKO mice (Fig. 7*C*); and 4) increased UCP1 protein (Fig. 7*D* and *SI Appendix*, Fig. S8*A*). Results from pWAT of cKO^{Atg7} mice less resembled those reported for aP2cKO^{Atg7} mice. Although reduced tissue weight for pWAT was consistent with those observed in aP2cKO^{Atg7} mice (Fig. 7*E*),

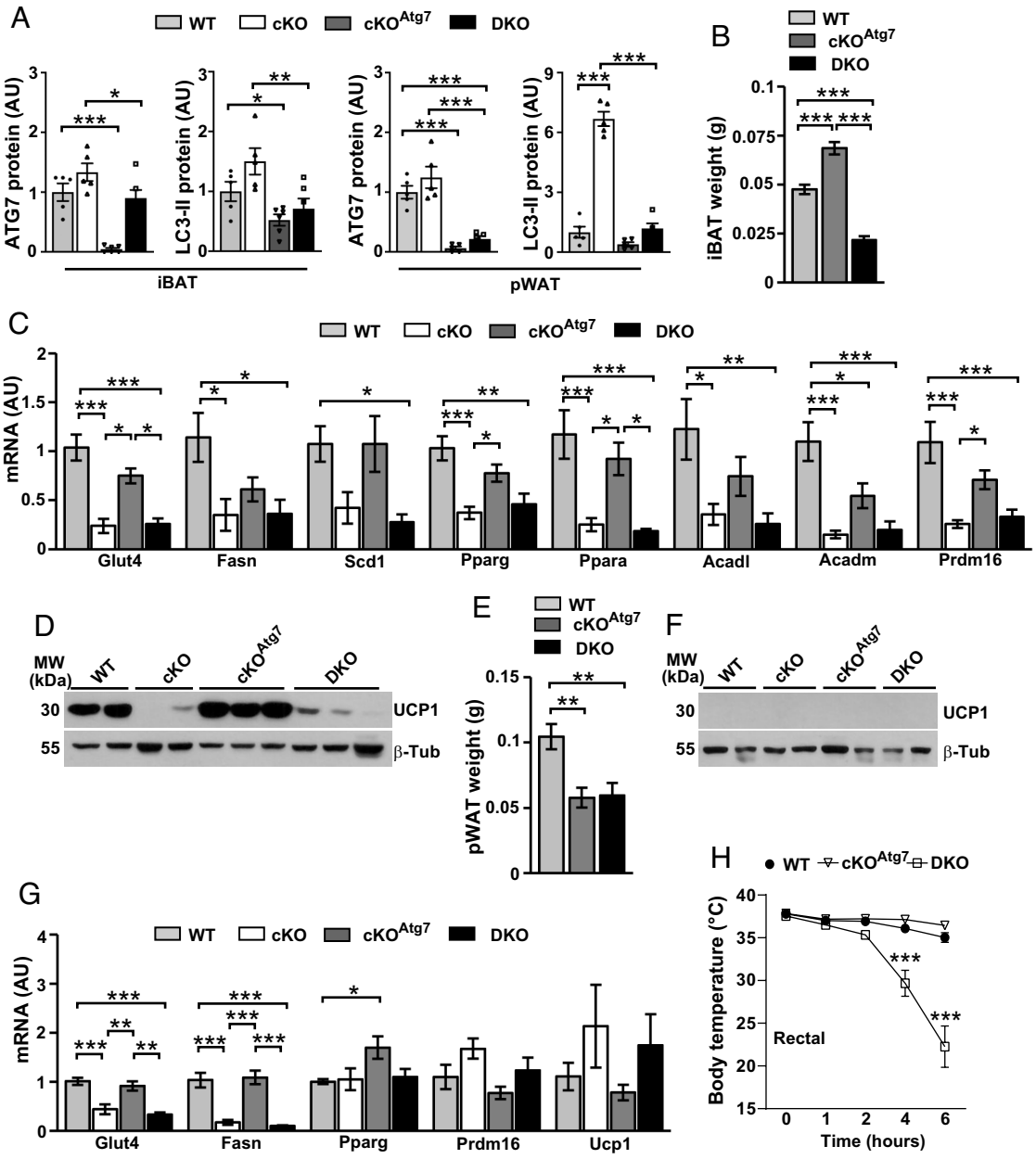

Fig. 7. Dominant phenotype of PIK3C3 deficiency over ATG7 deficiency in murine adipocytes. Mice (WT, wild-type; cKO, *Adipoq-Cre;Pik3c3*$^{f/f}$; cKO^{Atg7}, *Adipoq-Cre;Atg7*$^{f/f}$; DKO, *Adipoq-Cre;Pik3c3*$^{f/f}$;*Atg7*$^{f/f}$) at W8 were used. *A–D*. iBATs were examined for indicated proteins (*A*), tissue weight (*B*), indicated mRNAs (*C*), and UCP1 protein (*D*). *E–G*, pWATs were examined for tissue weight (*E*), UCP1 protein (*F*), and indicated mRNAs (*G*) with n = 4 to 7 in each group, except for tissue weight in which n = 9 to 18. *H*. Body temperature in response to cold and food deprivation was recorded (n = 4 in each group).

we did not detect any increase in either mRNA or protein for UCP1 (Fig. 7 *F* and *G* and *SI Appendix*, Fig. S8*A*). pWAT of cKO^{Atg7} mice contained more adipocytes of a smaller size (*SI Appendix*, Fig. S8*C*), and the expression levels of glucose transporter type 4 (*Glut4*), *Fasn*, and *Pparg* were preserved or enhanced (Fig. 7*G*). Therefore, *Adipoq-Cre*-mediated deletion of *Atg7* leads to a phenotype consistent with but less profound than aP2(*Fabp4*)-*Cre*-mediated *Atg7* deletion. Combined deficiency of PIK3C3 and ATG7 in DKO mice caused alterations in iBAT and pWAT that resembled those seen in cKO mice rather than in cKO^{Atg7} mice (Fig. 7). This was accompanied by a compromised ability to maintain body temperature under harsh conditions (Fig. 7*H*), at levels similar to those seen in cKO mice (Fig. 5*D*). Collectively, our findings indicate that PIK3C3 and ATG7 exert largely opposing effects on adipocytes, with a dominant role of PIK3C3 deficiency.

Dietary Lipid Excess Exacerbates AT Pathologies Yet Differentially Impacts Insulin and Glucose Tolerance in cKO Mice. Considering the abundance of diets rich in lipids, we evaluated how dietary lipid excess influences the outcome of PIK3C3 deficiency by feeding mice with a high-fat diet (HFD). Although food intake was higher, weight increase was lower in cKO mice and these mice also had smaller WAT depots at sacrifice (*SI Appendix*, Fig. S9*A*). Histologically, iBAT accumulated more lipids, whereas iWAT and pWAT appeared to contain more small-sized adipocytes compared to WT mice (*SI Appendix*, Fig. S9*B*). We measured selected markers for autophagy, lipid metabolism, thermogenesis, and apoptosis in iBAT and pWAT. PIK3C3 remained diminished and autophagy was disturbed in the two depots of cKO mice. PPARG, FASN, and perilipin (PLIN) in the two depots and UCP1 in iBAT were also significantly reduced. Apoptosis was accelerated in the two depots of cKO mice (*SI Appendix*,

Fig. S9*C*). We then examined metabolic parameters. Ectopic lipid deposition worsened compared to mice fed with chow diet (Fig. 2*E*) as hepatic steatosis was readily discernable on H&E-stained liver sections and liver weighed heavier in cKO mice (*SI Appendix*, Fig. S9*D*). cKO mice were nearly insulin unresponsive during IPITT (*SI Appendix*, Fig. S9*E*). However, despite the seemingly more severe pathology in ATs as well as liver and insulin resistance, cKO mice had lower blood glucose after 6 h fasting (*SI Appendix*, Fig. S9*E*) and lacked hyperglycemia after overnight fasting with lower blood glucose upon glucose challenge during IPGTT (*SI Appendix*, Fig. S9*F*). This is consistent with the divergence between insulin and glucose tolerance in chow-fed mice (Fig. 2 *A*–*C*) that became more evident upon HFD feeding, and reveals a better-preserved glucose tolerance in cKO mice.

Discussion

In this study, we have found that PIK3C3 functions in all adipocyte subsets and is crucial to the maintenance of BATs and WATs. Its absence impaired differentiation, survival, and function of adipocytes. This caused loss of WATs, whitening followed by loss of BATs, and impaired browning of WATs. Consequently, mice developed metabolic disorders manifested as dyslipidemia, hepatic steatosis, and insulin resistance. Compromised thermogenesis impaired the capacity of mice to maintain body temperature under extreme conditions. The effects of PIK3C3 largely opposed those of ATG7, and combined deficiency of both factors resembled the phenotype seen in PIK3C3 single-deficient mice. Finally, dietary lipid excess exacerbated pathologies caused by PIK3C3 deficiency in ATs and liver. These findings demonstrate a crucial role of PIK3C3 in maintaining healthy and functional ATs of all types and that *Pik3c3* deletion in mice causes metabolic disorders resembling lipodystrophy in humans. While the underlying mechanisms require further investigation, the reported findings indicate a differential impact of PIK3C3 on BATs and WATs.

We have found that mice with an adipocyte-specific PIK3C3 deficiency had a better-preserved glucose tolerance in the presence of insulin resistance, at least at the age examined. These mice also exhibited better-preserved glucose tolerance after HFD feeding for over 2 mo in the context of exacerbated pathologies in ATs and liver. These results are consistent with improved glucose tolerance found in 1- to 2-y-old mice carrying aP2(*Fabp4*)-*Cre*-mediated *Pik3c3* deletion (aP2cKO^{Pik3c3}) (36). Contrary to the latter model, we observed progressive deterioration of BATs and WATs in our model starting at a very young age accompanied by development of insulin resistance. It is unclear whether the off-target effects of aP2(*Fabp4*)-*Cre* in other organs explain this apparent discrepancy (48–50). The mechanism underlying the divergent effects of PIK3C3 deficiency on insulin sensitivity and glucose tolerance also remain unclear. It is intriguing to speculate that an altered secretome in ATs of these mice may impact other metabolic tissues involved in glycemic control (43, 51, 52), a possible scenario consistent with our analysis of circulating sRNAs and measurement of cytokines/adipokines in ATs. Alternatively, a regulatory circuit among ATs and other metabolic tissues could be at play that may change extracellular sRNA secretion from the latter tissues. Finally, PIK3C3 may differentially regulate cellular processes in adipocytes in an age-dependent manner. Together, the reported findings reveal a critical yet complex role for PIK3C3 in adipocytes.

Earlier studies on adipocyte autophagy prompted great enthusiasm for targeting this pathway for treatment of metabolic diseases (28–30). However, subsequent research revealed opposing effects of distinct autophagy factors on AT homeostasis and systemic metabolism (25–27). Hence, therapeutic strategies tailored towards individual factors will be needed for an optimal outcome. Understanding how each factor assumes its role will aid in such efforts. The functional level of each protein may also influence the metabolic outcome, exemplified by a previous study showing that partial inhibition of PIK3C3 improves insulin sensitivity and glycemic control (53).

PIK3C3 is an essential player in autophagosome formation and is also involved in endocytic sorting/trafficking (31–35). Our studies detected impaired autophagy in both PIK3C3-deficient primary ATs and differentiated preadipocyte cell lines. In the latter model, we did not observe significant alterations in endocytosis and vesicle trafficking. As such, our findings point toward autophagy as the more likely pathway responsible for the observed pathologies, but the exact contribution from defects in endocytic sorting/trafficking requires further investigation. The interplay between PIK3C3 and other autophagy proteins in adipocytes also requires further investigation. In our study, PIK3C3 deficiency caused alterations of P62, LC3-I, LC3-II, and LAMP1 in ATs, a pattern distinct from that of ATG7-deficient mice. The changes in LC3-II appeared ATG7-dependent, an observation consistent with previous findings in PIK3C3-deficient macrophages and embryonic fibroblasts (54, 55). Additionally, deletion of *Pik3c3* appeared to upregulate ATG7, and accumulation of LAMP1 was absent in ATG7-deficient mice. It will be of therapeutic interest to understand whether these distinct patterns underlie the opposing roles of PIK3C3 and ATG7 in adipocytes.

The current study demonstrates a critical yet complex role for adipocyte PIK3C3 in maintaining healthy ATs that largely opposes the impact of ATG7. The systemic consequences of PIK3C3 deficiency in mice closely resemble human lipodystrophy. Understanding the underlying mechanisms may identify molecules for therapeutic intervention in metabolic diseases.

Materials and Methods

Mice, reagents, metabolic parameters, tissue harvest and histology, cell preparation, collagen staining, flow cytometry, in vitro adipocyte differentiation, oxygen consumption, lipolysis assay, autophagy assays, endocytosis and vesicle trafficking assays, immortalized preadipocytes, Oil red O staining, real-time PCR, western blotting, tamoxifen treatment, body temperature and cold treatment, sympathetic nerve stimulation, HFD feeding, global untargeted lipidomics, sRNA sequencing and statistics are described in detail in *SI Appendix*.

Data, Materials, and Software Availability. All study data are included in the article and/or *SI Appendix*. Untargeted lipidomics data are included as Dataset S1 and are also available at the NIH Common Fund's National Metabolomics Data Repository (NMDR) website, the Metabolomics Workbench, https://www.metabolomicsworkbench.org under the assigned study ID: STST002268.

ACKNOWLEDGMENTS. This work was supported by NIH grants R01DK081536 (L.W. and L.V.K.), R01DK104817 (L.V.K.), R01AI139046 (L.V.K.), R01DK105550 (J.C.R.), K00CA234920 (J.B.), R01DK081646 (V.H.H), American Heart Association Grant 19TPA34910078 (L.V.K.), a discovery grant (to L.V.K.) from the Vanderbilt Diabetes Center (supported by P30DK020593), and the Vanderbilt O'Brien Kidney Center (P30DK114809). J.L.P. was supported by institutional training grants (T32HL069765 and T32AR059039). V.H.H was supported by the Krick-Brooks Chair in Nephrology. The study used the following resources at Vanderbilt University Medical Center (VUMC) supported by NIH grants P30CA068485, P30DK058404, and/or P30DK020593: Cell Imaging Shared Resource, Digital Histology Shared Resource, Translational Pathology Shared Resource, Mouse Metabolic Phenotyping Center, and Lipid Core. This work also used the resources of the Center for Innovative Technology (CIT) at Vanderbilt University.

Author affiliations: [a]Department of Pathology, Microbiology and Immunology, Vanderbilt University Medical Center, Nashville, TN 37232; [b]Department of Infectious Diseases and Public Health, City University of Hong Kong, Kowloon Tong 999077, Hong Kong; [c]Division of Epidemiology, Department of Medicine, Vanderbilt University Medical Center, Nashville, TN 37232; [d]Department of Biomedical Informatics, Vanderbilt University Medical Center, Nashville, TN 37232; [e]Division of Nephrology and Hypertension, Department of Medicine, Vanderbilt University Medical Center, Nashville, TN 37232; [f]The Vanderbilt O'Brien Kidney Center, Vanderbilt University Medical Center, Nashville, TN 37232; [g]Medical and Research Services, Department of Veterans Affairs Hospital, Tennessee Valley Healthcare System, Nashville, TN 37212; [h]Center for Innovative Technology, Vanderbilt University, Nashville, TN 37232; [i]Department of Chemistry, Vanderbilt University, Nashville, TN 37232; [j]Department of Pathology, University of Alabama at Birmingham, Birmingham, AL 35294; and [k]Birmingham Veterans Affairs Medical Center, Birmingham, AL 35233

1. R. K. Zwick, C. F. Guerrero-Juarez, V. Horsley, M. V. Plikus, Anatomical, physiological, and functional diversity of adipose tissue. *Cell Metab.* **27**, 68–83 (2018).
2. E. D. Rosen, B. M. Spiegelman, What we talk about when we talk about fat. *Cell* **156**, 20–44 (2014).
3. E. E. Kershaw, J. S. Flier, Adipose tissue as an endocrine organ. *J. Clin. Endocrinol. Metab.* **89**, 2548–2556 (2004).
4. S. Kita, N. Maeda, I. Shimomura, Interorgan communication by exosomes, adipose tissue, and adiponectin in metabolic syndrome. *J. Clin. Invest.* **129**, 4041–4049 (2019).
5. L. Scheja, J. Heeren, The endocrine function of adipose tissues in health and cardiometabolic disease. *Nat. Rev. Endocrinol.* **15**, 507–524 (2019).
6. C. R. Kahn, G. Wang, K. Y. Lee, Altered adipose tissue and adipocyte function in the pathogenesis of metabolic syndrome. *J. Clin. Invest.* **129**, 3990–4000 (2019).
7. A. L. Ghaben, P. E. Scherer, Adipogenesis and metabolic health. *Nat. Rev. Mol. Cell Biol.* **20**, 242–258 (2019).
8. J. M. Rutkowski, J. H. Stern, P. E. Scherer, The cell biology of fat expansion. *J. Cell Biol.* **208**, 501–512 (2015).
9. U. White, E. Ravussin, Dynamics of adipose tissue turnover in human metabolic health and disease. *Diabetologia* **62**, 17–23 (2019).
10. M. Shao *et al.*, Cellular origins of beige fat cells revisited. *Diabetes* **68**, 1874–1885 (2019).
11. W. Wang, P. Seale, Control of brown and beige fat development. *Nat. Rev. Mol. Cell Biol.* **17**, 691–702 (2016).
12. J. P. Mann, D. B. Savage, What lipodystrophies teach us about the metabolic syndrome. *J. Clin. Invest.* **129**, 4009–4021 (2019).
13. C. G. Fiorenza, S. H. Chou, C. S. Mantzoros, Lipodystrophy: Pathophysiology and advances in treatment. *Nat. Rev. Endocrinol.* **7**, 137–150 (2011).
14. R. J. Brown *et al.*, The diagnosis and management of lipodystrophy syndromes: A multi-society practice guideline. *J. Clin. Endocrinol. Metab.* **101**, 4500–4511 (2016).
15. M. Torriani *et al.*, Dysfunctional subcutaneous fat with reduced dicer and brown adipose tissue gene expression in HIV-infected patients. *J. Clin. Endocrinol. Metab.* **101**, 1225–1234 (2016).
16. R. Cereijo *et al.*, The molecular signature of HIV-1-associated lipomatosis reveals differential involvement of brown and beige/brite adipocyte cell lineages. *PLoS One* **10**, e0136571 (2015).
17. C. Pellegrini *et al.*, Altered adipocyte differentiation and unbalanced autophagy in type 2 familial partial lipodystrophy: An in vitro and in vivo study of adipose tissue browning. *Exp. Mol. Med.* **51**, 1–17 (2019).
18. N. Mizushima, M. Komatsu, Autophagy: Renovation of cells and tissues. *Cell* **147**, 728–741 (2011).
19. V. Lahiri, W. D. Hawkins, D. J. Klionsky, Watch what you (self-) eat: Autophagic mechanisms that modulate metabolism. *Cell Metab.* **29**, 803–826 (2019).
20. M. B. Khawar, H. Gao, W. Li, Autophagy and lipid metabolism. *Adv. Exp. Med. Biol.* **1206**, 359–374 (2019).
21. J. New, S. M. Thomas, Autophagy-dependent secretion: Mechanism, factors secreted, and disease implications. *Autophagy* **15**, 1682–1693 (2019).
22. M. Onishi, K. Yamano, M. Sato, N. Matsuda, K. Okamoto, Molecular mechanisms and physiological functions of mitophagy. *EMBO J.* **40**, e104705 (2021).
23. I. Dikic, Z. Elazar, Mechanism and medical implications of mammalian autophagy. *Nat. Rev. Mol. Cell Biol.* **19**, 349–364 (2018).
24. B. Levine, G. Kroemer, Biological functions of autophagy genes: A disease perspective. *Cell* **176**, 11–42 (2019).
25. Y. Jin *et al.*, Depletion of adipocyte Becn1 leads to lipodystrophy and metabolic dysregulation. *Diabetes* **70**, 182–195 (2021).
26. T. Yamamuro *et al.*, Age-dependent loss of adipose Rubicon promotes metabolic disorders via excess autophagy. *Nat. Commun.* **11**, 4150 (2020).
27. J. Cai *et al.*, Autophagy ablation in adipocytes induces insulin resistance and reveals roles for lipid peroxide and Nrf2 signaling in adipose-liver crosstalk. *Cell Rep.* **25**, 1708–1717.e1705 (2018).
28. S. Altshuler-Keylin *et al.*, Beige adipocyte maintenance is regulated by autophagy-induced mitochondrial clearance. *Cell Metab.* **24**, 402–419 (2016).
29. R. Singh *et al.*, Autophagy regulates adipose mass and differentiation in mice. *J. Clin. Invest.* **119**, 3329–3339 (2009).
30. Y. Zhang *et al.*, Adipose-specific deletion of autophagy-related gene 7 (atg7) in mice reveals a role in adipogenesis. *Proc. Natl. Acad. Sci. U.S.A.* **106**, 19860–19865 (2009).
31. A. Kihara, T. Noda, N. Ishihara, Y. Ohsumia, Two distinct Vps34 phosphatidylinositol 3–kinase complexes function in autophagy and carboxypeptidase Y sorting in Saccharomyces cerevisiae. *J. Cell Biol.* **152**, 519–530 (2001).
32. E. Itakura, C. Kishi, K. Inoue, N. Mizushima, Beclin 1 forms two distinct phosphatidylinositol 3-kinase complexes with mammalian Atg14 and UVRAG. *Mol. Biol. Cell* **19**, 5360–5372 (2008).
33. C. Liang *et al.*, Beclin1-binding UVRAG targets the class C Vps complex to coordinate autophagosome maturation and endocytic trafficking. *Nat. Cell Biol.* **10**, 776–787 (2008).
34. L. Galluzzi, D. R. Green, Autophagy-independent functions of the autophagy machinery. *Cell* **177**, 1682–1699 (2019).
35. J. M. Backer, The intricate regulation and complex functions of the class III phosphoinositide 3-kinase Vps34. *Biochem J.* **473**, 2251–2271 (2016).
36. A. K. Ghosh, T. Mau, M. O'Brien, R. Yung, Novel role of autophagy-associated Pik3c3 gene in gonadal white adipose tissue browning in aged C57/Bl6 male mice. *Aging* **10**, 764–774 (2018).
37. K. Y. Lee *et al.*, Lessons on conditional gene targeting in mouse adipose tissue. *Diabetes* **62**, 864–874 (2013).
38. M. S. Rodeheffer, K. Birsoy, J. M. Friedman, Identification of white adipocyte progenitor cells in vivo. *Cell* **135**, 240–249 (2008).
39. J. Moitra *et al.*, Life without white fat: A transgenic mouse. *Genes, Dev.* **12**, 3168–3181 (1998).
40. S. R. Farmer, Transcriptional control of adipocyte formation. *Cell Metab.* **4**, 263–273 (2006).
41. P. Seale *et al.*, Transcriptional control of brown fat determination by PRDM16. *Cell Metab.* **6**, 38–54 (2007).
42. P. Cohen *et al.*, Ablation of PRDM16 and beige adipose causes metabolic dysfunction and a subcutaneous to visceral fat switch. *Cell* **156**, 304–316 (2014).
43. J. Funcke, P. E. Scherer, Beyond adiponectin and leptin: Adipose tissue-derived mediators of inter-organ communication. *J. Lipid Res.* **60**, 1648–1697 (2019).
44. E. T. Chouchani, L. Kazak, B. M. Spiegelman, New advances in adaptive thermogenesis: UCP1 and beyond. *Cell Metab.* **29**, 27–37 (2019).
45. B. B. Lowell, B. M. Spiegelman, Towards a molecular understanding of adaptive thermogenesis. *Nature* **404**, 652–660 (2000).
46. N. Mizushima, T. Yoshimori, How to interpret LC3 immunoblotting. *Autophagy* **3**, 542–545 (2007).
47. J. G. Granneman, P. Li, Z. Zhu, Y. Lu, Metabolic and cellular plasticity in white adipose tissue I: Effects of beta3-adrenergic receptor activation. *Am. J. Physiol. Endocrinol. Metab.* **289**, E608–616 (2005).
48. S. E. Mullican, A novel adipose-specific gene deletion model demonstrates potential pitfalls of existing methods. *Mol. Endocrinol.* **27**, 127–134 (2013).
49. E. Harno, E. C. Cottrell, A. White, Metabolic pitfalls of CNS Cre-based technology. *Cell Metab.* **18**, 21–28 (2013).
50. K. Martens, A. Bottelbergs, M. Baes, Ectopic recombination in the central and peripheral nervous system by aP2/FABP4-Cre mice: Implications for metabolism research. *FEBS Lett.* **584**, 1054–1058 (2010).
51. I. Gesmundo *et al.*, Adipocyte-derived extracellular vesicles regulate survival and function of pancreatic β cells. *JCI Insight* **6**, e141962 (2021).
52. T. Thomou *et al.*, Adipose-derived circulating miRNAs regulate gene expression in other tissues. *Nature* **542**, 450–455 (2017).
53. B. Bilanges *et al.*, Vps34 PI 3-kinase inactivation enhances insulin sensitivity through reprogramming of mitochondrial metabolism. *Nat. Commun.* **8**, 1804 (2017).
54. N. Jaber *et al.*, Class III PI3K Vps34 plays an essential role in autophagy and in heart and liver function. *Proc. Natl. Acad. Sci. U.S.A.* **109**, 2003–2008 (2012).
55. G. Yang *et al.*, Pik3c3 deficiency in myeloid cells imparts partial resistance to experimental autoimmune encephalomyelitis associated with reduced IL-1β production. *Cell Mol. Immunol.* **18**, 2024–2039 (2020).